THE HALF-PLANES PROBLEM FOR THE LEVEL SET EQUATION

STÉPHANE CLAIN AND MALCOM DJENNO NGOMANDA

Abstract.   The paper is dedicated to the construction of an analytic solution for the level set equation in $\mathbb{R}^2$ with an initial condition constituted by two half-planes. Such a problem can be seen as an equivalent Riemann problem in the Hamilton-Jacobi equation context. We first rewrite the level set equation as a non-strictly hyperbolic problem and obtain a Riemann problem where the line sharing the initial discontinuity corresponds to the half-planes junction. Three different solutions corresponding to a shock, a rarefaction and a contact discontinuity are given in function of the two half-planes configuration and we derive the solution for the level set equation. The study provides theoretical examples to test the numerical methods approaching the solution of viscosity of the level set equation. We perform simulations to check the three situations using a classical numerical method on a structured grid.

Key Words. Riemann problem, Cauchy problem, level set equation, analytical solution, half-planes problem

1. Introduction

The interface tracking problem takes place in various fields like front flame propagation, crystal growth in solidification process, fluid-structure interaction with moving solid boundary, computer vision, dynamics bubbles or drops for example. The level set method (see [8] for an overview) consists in representing the free boundary as the zero-level of a continuous function ϕ where the normal velocity F is a prescribed function.
Consider the Cauchy problem:

$$(1) \qquad \begin{cases} \partial_t \phi(\boldsymbol{x},t) + F\,|\nabla\phi(\boldsymbol{x},t)| = 0 & \text{in } \mathbb{R}^2 \times [0,T], \\ \phi(\boldsymbol{x},t=0) = \phi_0(\boldsymbol{x}) & \text{in } \mathbb{R}^2, \end{cases}$$

where $F(\boldsymbol{x},t)$ is a given Lipschitz function on $\mathbb{R}^2 \times [0,T]$ while ϕ_0 is a Lipschitz function on $\mathbb{R}^2$. Existence and uniqueness of the Lipschitz viscosity solution for problem (1) on $\mathbb{R}^2 \times [0,T]$ is proved (see [1, 7]).
Since ϕ is a Lipschitz function, vector $\mathbf{U} = \nabla\phi$ is a bounded vector-valued function and applying the gradient operator to equation (1), we derive the Cauchy problem for the conservation law system associated to the level set equation:

$$(2) \qquad \begin{cases} \partial_t \mathbf{U}(\boldsymbol{x},t) + \nabla(F\,|\mathbf{U}(\boldsymbol{x},t)|) = 0 & \text{in } \mathbb{R}^2 \times [0,T], \\ \mathbf{U}(\boldsymbol{x},t=0) = \nabla\phi_0(\boldsymbol{x}) & \text{in } \mathbb{R}^2. \end{cases}$$

For the one dimensional situation, [7] proves that the Lipschitz viscosity solution ϕ of equation (1) corresponds to the bounded entropic solution U of equation (2) with $U = \partial_x \phi$. Such a result is not established for higher dimension since we do not have the uniqueness of solution for the non-strictly hyperbolic system (2) [2]. Nevertheless, if we regularize equations (1) and (2) adding a diffusion term $\varepsilon\Delta\phi$ and $\varepsilon\Delta U$ respectively, the new solutions satisfy $\mathbf{U}_\varepsilon = \nabla\phi_\varepsilon$. Passing to the limit assuming a L^∞ convergence of ϕ_ε

toward ϕ and a L^1 convergence of U_ε toward U, we have that $\mathbf{U} = \nabla\phi$ where ϕ is the viscosity solution and U the entropy solution.

From a numerical point of view, the non-strictly hyperbolic system discretization using the finite volume method leads to solve Riemann problems for each cell interface. The problem is reduced to a one dimensional hyperbolic equation with a discontinuous flux function [3] making difficult a complete and explicit resolution. We propose a different approach based on the following remark: a constant state for the non-strictly hyperbolic problem (2) corresponds to a plane for the level set equation (1). Hence we propose to study an equivalent Riemann problem in the level set equation context using two half-planes as an initial continuous condition [4, 5].

2. The two half-planes problem

For the sake of simplicity, we assume in the following that function F is reduced to a constant function. Such an assumption is not restrictive since we usually solve Riemann problems using the normal velocity evaluated at the interface midpoint.
Let π_1 and π_2 be two planes of the $(\boldsymbol{x}, z) = (x_1, x_2, z) \in \mathbb{R}^3$ space. We impose that the planes contain the origin point and the plane equations write

$$z = \phi_i(\boldsymbol{x}) = \mathbf{U}_i.\boldsymbol{x}, \quad i = 1, 2$$

where $\mathbf{U}_i$ are given vectors of $\mathbb{R}^2$. Of course, when the two planes are equal, one has $\phi_0(\boldsymbol{x}) = \phi_1(\boldsymbol{x}) = \phi_2(\boldsymbol{x})$ as an initial condition and the solution is given by $\phi(\boldsymbol{x}, t) = \phi_0(\boldsymbol{x}) - F|\mathbf{U}_L|t$ with $\mathbf{U}_L = \mathbf{U}_1 = \mathbf{U}_2$ which corresponds to a simple translation of the initial plane with velocity $F|\boldsymbol{U}_L|$ (see figure (1)).
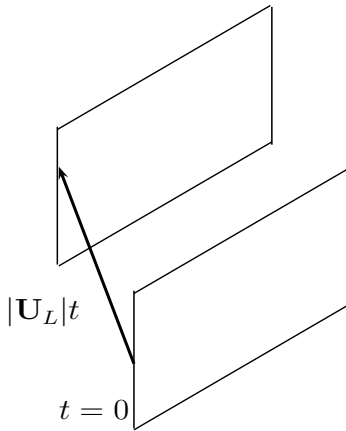

Figure 1: *The trivial case when $\phi_0 = \phi_1 = \phi_2$. The solution representation in $\mathbb{R}^3$ corresponds to the initial plane translated following the Oz axis with velocity $F|\boldsymbol{U}_L| = F|\nabla\phi_0|$ (we take $F = 1$ in the figure).*

Now, we consider the nontrivial case when the two planes are different. To construct an initial condition ϕ_0 for the Cauchy problem (1) we consider an arbitrary line $\delta \subset \mathbb{R}^2$ passing to the origin, an arbitrary normal vector $\mathbf{W} \in \mathbb{R}^2$ and we define the left part $\mathcal{P}_L$ and the right part $\mathcal{P}_R$ of $\mathbb{R}^2$ such that $\mathbf{W}$ goes from left to right (see figure (2)). We then construct the initial condition by $\phi_0(\boldsymbol{x}) = \phi_1(\boldsymbol{x})$ if $\boldsymbol{x} \in \mathcal{P}_L$ and $\phi_0(\boldsymbol{x}) = \phi_2(\boldsymbol{x})$ if $\boldsymbol{x} \in \mathcal{P}_R$. Such a definition gives rise to a function which is not *a priori* continuous on δ and disqualify the construction since we would like to handle continuous solutions. It results that the interface δ can not be arbitrary but has to be defined such that we have a

continuous connection between the two planes. To this end, we introduce the two following continuous Lipschitz functions

$$\phi_0^m = \min(\phi_1, \phi_2), \qquad \phi_0^M = \max(\phi_1, \phi_2)$$

which are the unique function linking π_1 with π_2 continuously. Note that the particular case $\mathbf{U}_1 = \mathbf{U}_2$ corresponds to a unique function $\phi_0^m = \phi_0^M = \phi_1 = \phi_2$.

Assuming $\mathbf{U}_1 \neq \mathbf{U}_2$, we set

$$\mathbf{W} = \frac{\mathbf{U}_1 - \mathbf{U}_2}{|\mathbf{U}_1 - \mathbf{U}_2|}$$

and define the two half-planes $\mathcal{P}_L$ and $\mathcal{P}_R$ of $\mathbb{R}^2$ by

$$\mathcal{P}_L = \{\boldsymbol{x} \in \mathbb{R}^2; \ \boldsymbol{x}.\mathbf{W} < 0\}, \quad \mathcal{P}_R = \{\boldsymbol{x} \in \mathbb{R}^2; \ \boldsymbol{x}.\mathbf{W} > 0\}.$$

The line $\delta_c = \overline{\mathcal{P}_L} \cap \overline{\mathcal{P}_R}$ is orthogonal to $\mathbf{W}$ and we choose the unit vector $\mathbf{V}$ on δ_c such that the vectors $\{\mathbf{W}, \mathbf{V}\}$ form a direct orthonormal basis of $\mathbb{R}^2$ (see figure (2)). Note that by construction $\mathbf{W}$ goes from $\mathcal{P}_L$ to $\mathcal{P}_R$.
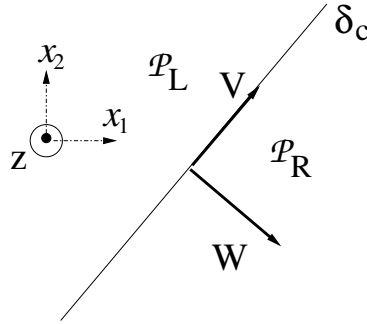

Figure 2: Orientation and definition of $\mathcal{P}_L$ and $\mathcal{P}_R$.

In $\mathbb{R}^3$, the two planes π_1 and π_2 have an intersection line $\Delta_c = \pi_1 \cap \pi_2 \subset \mathbb{R}^3$ passing by the origin O and $\delta_c \subset \mathbb{R}^2$ is the orthogonal projection of line $\Delta_c \subset \mathbb{R}^3$ on the plane (x_1, x_2) (see figure (3)).
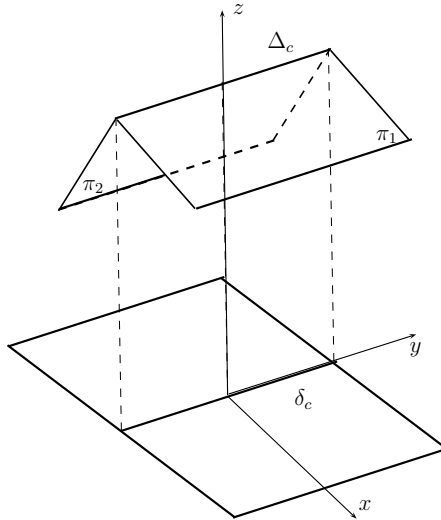

Figure 3: Representation of function ϕ_0^m in $\mathbb{R}^3$. The two half-planes intersection provides the line Δ_c which the orthogonal projection on (x_1, x_2) corresponds to line δc.

We now aim to study the Cauchy problem (1) using ϕ_0^m or ϕ_0^M as an initial condition. In the hyperbolic context, we have to consider Riemann problems (2) where the initial conditions are $\nabla\phi_0^m$ or $\nabla\phi_0^M$ with a discontinuity situated on the line δ_c. Two cases arise whether we choose ϕ_0^m or ϕ_0^M as an initial condition.

- If ϕ_0^m is the initial condition, definition of $\mathbf{W}$ yields that $\phi_0^m = \phi_1$ on the half-plane $\mathcal{P}_L$ and $\phi_0^m = \phi_2$ on the half-plane $\mathcal{P}_R$. Indeed, we have $\mathbf{W}.\mathbf{W} = 1 > 0$ so $(\mathbf{U}_1 - \mathbf{U}_2).\mathbf{W} > 0$ then $\mathbf{U}_1.\mathbf{W} > \mathbf{U}_2.\mathbf{W}$ which means that $\phi_1(\mathbf{W}) > \phi_2(\mathbf{W})$. Hence π_1 is above π_2 on $\mathcal{P}_R$ while π_1 is under π_2 on $\mathcal{P}_L$. In the conservative law framework, we derive the following initial condition for the Riemann problem $\mathbf{U}_L = \mathbf{U}_1$ on $\mathcal{P}_L$ and $\mathbf{U}_R = \mathbf{U}_2$ on $\mathcal{P}_R$.
- If we choose ϕ_0^M as the initial condition, we deduce that $\mathbf{U}_L = \mathbf{U}_2$ on $\mathcal{P}_L$ and $\mathbf{U}_R = \mathbf{U}_1$ on $\mathcal{P}_R$.

In the sequel, for any arbitrary couple of vectors $\mathbf{U}_1$ and $\mathbf{U}_2$ we choose ϕ_0^m as the initial condition and we have $\mathbf{U}_L = \mathbf{U}_1$ on $\mathcal{P}_L$ and $\mathbf{U}_R = \mathbf{U}_2$ on $\mathcal{P}_R$ oriented from left to right by

$$(3) \qquad \mathbf{W} = \frac{\mathbf{U}_L - \mathbf{U}_R}{|\mathbf{U}_L - \mathbf{U}_R|}.$$

2.1. The one dimensional problem reduction. The objective is to determine the theoretical solution ϕ of the level set equation with ϕ_0^m as an initial condition using the solution $\mathbf{U}$ of the associated Riemann problem. To this end, we carry out the following change of variable where we introduce the coordinates in basis $\{\mathbf{W}, \mathbf{V}\}$ setting

$$\boldsymbol{x} = \zeta\mathbf{W} + \eta\mathbf{V}.$$

The transformation corresponds to a rotation in the new basis where

$$\mathbf{W} = \begin{pmatrix} 1 \\ 0 \end{pmatrix}, \quad \mathbf{V} = \begin{pmatrix} 0 \\ 1 \end{pmatrix}.$$

By construction of $\mathbf{V}$ and $\mathbf{W}$ we have $\mathbf{U}_L \cdot \mathbf{V} = \mathbf{U}_R \cdot \mathbf{V} = \omega_0$, thus, vectors $\mathbf{U}_L$ and $\mathbf{U}_R$ are defined in the new base:

$$\mathbf{U}_L = \omega_L\mathbf{W} + \omega_0\mathbf{V}, \quad \mathbf{U}_R = \omega_R\mathbf{W} + \omega_0\mathbf{V},$$

with $\omega_L = \mathbf{U}_L \cdot \mathbf{W}$, $\omega_R = \mathbf{U}_R \cdot \mathbf{W}$.

Using the change of variables, the level set problem becomes

$$(4) \qquad \begin{cases} \partial_t\phi(\zeta,\eta,t) + F\,|\nabla_{\zeta,\eta}\phi(\zeta,\eta,t)| = 0, \\ \phi(\zeta,\eta) = \omega_L\zeta + \omega_0\eta \quad \text{if } \zeta < 0, \quad \eta \in \mathbb{R}, \\ \phi(\zeta,\eta) = \omega_R\zeta + \omega_0\eta \quad \text{if } \zeta > 0, \quad \eta \in \mathbb{R}, \end{cases}$$

and the associated Riemann problem:

$$(5) \qquad \begin{cases} \partial_t\mathbf{U}(\zeta,\eta,t) + \nabla_{\zeta,\eta}\left(F\,|\mathbf{U}(\zeta,\eta,t)|\right) = 0, \\ \\ \mathbf{U}(.,0) = \begin{pmatrix} \omega_L \\ \omega_0 \end{pmatrix} \quad \text{if } \zeta < 0, \quad \eta \in \mathbb{R}, \\ \\ \mathbf{U}(.,0) = \begin{pmatrix} \omega_R \\ \omega_0 \end{pmatrix} \quad \text{if } \zeta > 0, \quad \eta \in \mathbb{R}, \end{cases}$$

If $\mathbf{U}(\zeta, \eta, t)$ is a solution of (5) then $\mathbf{U}(\zeta, \eta + c, t)$ is also a solution of (5) for all $c \in \mathbb{R}$ thus $\mathbf{U}(\zeta, \eta + c, t) = \mathbf{U}(\zeta, \eta, t)$ hence $\partial_\eta \mathbf{U} = 0$. It follows that

$$\partial_t \mathbf{U}(\zeta, t) \cdot \begin{pmatrix} 0 \\ 1 \end{pmatrix} = 0$$

hence $\mathbf{U} \cdot \begin{pmatrix} 0 \\ 1 \end{pmatrix} = \omega_0, \forall \eta, \zeta, t$.

On the other hand, let $\omega(\zeta, t) = \mathbf{U} \cdot \begin{pmatrix} 1 \\ 0 \end{pmatrix}$, the component of $\mathbf{U}$ following the direction W, function ω satisfy the one-dimension scalar Riemann problem

(6) $$\begin{cases} \partial_t \omega(\zeta, t) + F \partial_\zeta \sqrt{w^2(\zeta, t) + w_0^2} = 0, \\ \omega(\zeta, 0) = \omega_L, \zeta < 0, \\ \omega(\zeta, 0) = \omega_R, \zeta > 0. \end{cases}$$

Note that the choice of $\mathbf{W}$ yields $\mathbf{U}_L.\mathbf{W} > \mathbf{U}_R.\mathbf{W}$ hence $\omega_L \geq \omega_R$.

3. Solutions for the Riemann problem

We first give the solution for the situation $\omega_0 \neq 0$, case $\omega_0 = 0$ will be studied as the limit situation when ω_0 tends to 0. We denote by $f(\omega) = F\sqrt{w^2 + w_0^2}$, and a simple calculation provides

$$\lambda(\omega) = f'(\omega) = \frac{F\omega}{\sqrt{w^2 + w_0^2}}, \qquad f''(\omega) = \frac{Fw_0^2}{(w^2 + w_0^2)^{\frac{3}{2}}}.$$

We note that f' is an increasing function for $F \geq 0$ while f' is a decreasing function if $F \leq 0$. Since $\omega_L > \omega_R$ it result that $\lambda(\omega_L) > \lambda(\omega_R)$ if $F > 0$ leading to an entropic shock configuration while $\lambda(\omega_L) < \lambda(\omega_R)$ if $F < 0$ which corresponds to a rarefaction [6].

3.1. The shock case $F \geq 0$. We first assume $\omega_0 \neq 0$. The Rankine-Hugoniot condition yields

(7) $$\sigma = \frac{f(\omega_L) - f(\omega_R)}{\omega_L - \omega_R} = F\frac{|\mathbf{U}_L| - |\mathbf{U}_R|}{|\mathbf{U}_L - \mathbf{U}_R|}.$$
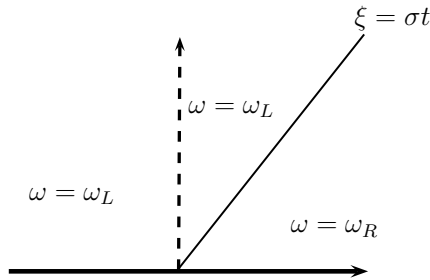

Figure 4: Shock wave, case $\omega_0 \neq 0$

We now consider the case where $\omega_0 = 0$ with $\omega_L \neq \omega_R$. Such a situation arises when vectors $\mathbf{U}_L$ and $\mathbf{U}_R$ are collinear. Since $\omega_L \neq \omega_R$, then we can pass to the limit setting $\omega_0 = 0$ in relation (7) since f depends continuously on ω_0. The solution is still an entropic shock.

3.2. The rarefaction case $F < 0$. We first assume that $\omega_0 \neq 0$ and we seek for an auto-similar solution which satisfies

$$(8) \qquad f'(\omega(\zeta, t)) = \frac{\zeta}{t}.$$

Since $f''(\omega) < 0$, we deduce that $f'(\omega)$ is a one-to-one function mapping $\mathbb{R}$ onto $]F, -F[$ and $F < \lambda(\omega_L) < \lambda(\omega_R) < -F$ since $\omega_L > \omega_R$. From relation (8), we deduce

$$F^2 \omega^2 = \left(\frac{\zeta}{t}\right)^2 (\omega^2 + \omega_0^2),$$

and we get an explicit expression of ω in the fan

$$(9) \qquad \omega(\zeta, t) = -\frac{\frac{\zeta}{t}|\omega_0|}{\sqrt{F^2 - \left(\frac{\zeta}{t}\right)^2}}, \qquad \frac{\zeta}{t} \in]\lambda(\omega_L), \lambda(\omega_R)[.$$

Three cases arise in function of the ω_L and ω_R signs that we display in figure (5).

(1) If $\omega_L > \omega_R \geq 0$ then $f'(\omega_L) < f'(\omega_R) \leq 0$: the fan is contained in the left half-plane $\mathcal{P}_L$ and the flux on interface δ_c is $F|U_R|$.

(2) If $0 \geq \omega_L > \omega_R$ then $0 \leq f'(\omega_L) < f'(\omega_R)$: the fan is contained in the right half-plane $\mathcal{P}_R$ and the flux on interface δ_c is $F|U_L|$.

(3) At last, if $\omega_L > 0 > \omega_R$ then $f'(\omega_L) < 0 < f'(\omega_R)$, the fan crosses the line δ_c and the flux on the interface line δ_c is $F|\omega_0|$.
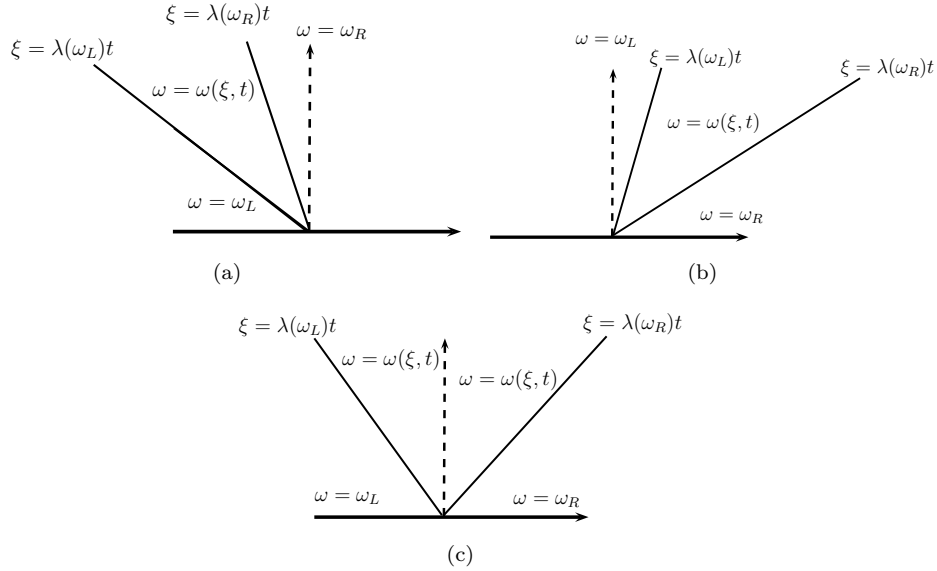

Figure 5: Rarefaction situations with $\omega_0 \neq 0$. Three cases arise in function of ω_L and ω_L signs: $\omega_R > 0$ (a), $0 > \omega_L$ (b), $\omega_L > 0 > \omega_R$ (c).

We now consider the situation when ω_0 vanishes. For all parameters $\omega_0 \neq 0$, function $f'(\omega; \omega_0) = \lambda(\omega; \omega_0)$ is a one-to-one function of ω from $\mathbb{R}$ onto $]F, -F[$ and the rarefaction takes place between $\lambda(\omega_L; \omega_0)$ and $\lambda(\omega_R; \omega_0)$. For ω_L and ω_R fixed, we take the limit $\omega_0 \to 0$ and we have

$$\lim_{\omega_0 \to 0} \lambda(\omega_i, \omega_0) = -F, \text{ if } \omega_i < 0, \qquad \lim_{\omega_0 \to 0} \lambda(\omega_i; \omega_0) = +F, \text{ if } \omega_i > 0$$

with $i = L, R$. In addition, relation (9) says

$$\lim_{\omega_0 \to 0} w(\zeta, t) = 0, \quad \forall \zeta \in]F, -F[, t > 0.$$

Three cases again then arise.

(1) If $\omega_L > \omega_R > 0$ then $\lim_{\omega_0 \to 0} \lambda(\omega_L, \omega_0) = \lim_{\omega_0 \to 0} \lambda(\omega_R, \omega_0) = +F < 0$ and the rarefaction is reduced to a contact discontinuity moving with the velocity $\sigma = +F$ (see figure (6-a)).

(2) If $0 > \omega_L < \omega_R$ then $\lim_{\omega_0 \to 0} \lambda(\omega_L, \omega_0) = \lim_{\omega_0 \to 0} \lambda(\omega_R, \omega_0) = -F > 0$ and the rarefaction is reduced to a contact discontinuity moving with the velocity $\sigma = -F$ (see figure (6-b)).

(3) At last, if $\omega_L > 0 > \omega_R$ then $\lim_{\omega_0 \to 0} \lambda(\omega_L, \omega_0) = +F$, $\lim_{\omega_0 \to 0} \lambda(\omega_R, \omega_0) = -F$ and the rarefaction is reduced to the null solution in the cone $F < \frac{\zeta}{t} < -F$ (see figure (6-c)).
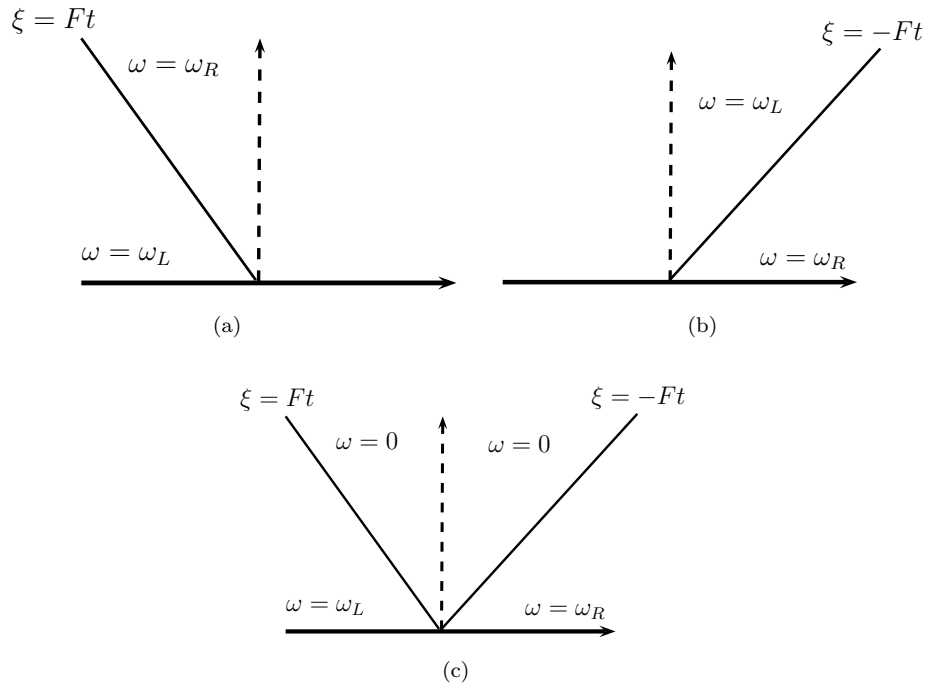

Figure 6: The rarefaction degenerates into a contact discontinuity when $\omega_0 = 0$. Three situations arise in function of ω_L and ω_R signs: $\omega_L < 0$ (a), $0 < \omega_R$ (b), $\omega_R < 0 < \omega_L$ (c).

Remark 3.1. *Two other cases arise whether $\omega_L = 0$ case (i) or $\omega_R = 0$ case (ii). This particular situation is similar to case (c) but the rarefaction cone is reduced to the left half-cone $]F, 0]$ in case (i) and the right half-cone $[0, -F[$ in case (ii).*

4. Solution for the level set equation

Based on the solution obtained with the Riemann problem, we build the solution for the level set equation. We distinguish the cases whether F is positive or negative.

4.1. The shock: case $F > 0$. For $t \geq 0$, we define the line $\delta_c(t)$ parallel to $\delta_c(0) = \delta_c$ moving with the velocity

$$\sigma = F \frac{|\mathbf{U}_g| - |\mathbf{U}_d|}{|\mathbf{U}_g - \mathbf{U}_d|}.$$

i.e. $\delta_c(t) = \{\boldsymbol{x} \in \mathbb{R}^2; \ \mathbf{W}.\boldsymbol{x} = \sigma t\}$. We then consider the two half-planes situated on the left and right side of $\delta_c(t)$ (see figure 7)

$$\mathcal{P}_L(t) = \{\boldsymbol{x} \in \mathbb{R}^2; \ \boldsymbol{x}.\mathbf{W} < \sigma t\}, \qquad \mathcal{P}_R(t) = \{\boldsymbol{x} \in \mathbb{R}^2; \ \boldsymbol{x}.\mathbf{W} > \sigma t\}.$$

From section 3.1, the solution $\mathbf{U}(\boldsymbol{x}, t)$ of the Riemann problem (2) is given by

$$\mathbf{U}(\boldsymbol{x}, t) = \mathbf{U}_L, \quad \boldsymbol{x} \in \mathcal{P}_L(t),$$
$$\mathbf{U}(\boldsymbol{x}, t) = \mathbf{U}_R, \quad \boldsymbol{x} \in \mathcal{P}_R(t).$$

We then define

$$\phi(\boldsymbol{x}, t) = \boldsymbol{x}.\mathbf{U}_L - F\,|\mathbf{U}_L|\,t, \quad \boldsymbol{x} \in \mathcal{P}_L(t),$$
$$\phi(\boldsymbol{x}, t) = \boldsymbol{x}.\mathbf{U}_R - F\,|\mathbf{U}_R|\,t, \quad \boldsymbol{x} \in \mathcal{P}_R(t).$$

We easily check that ϕ is a continuous function thanks to the shock velocity definition and $\nabla\phi = \mathbf{U}$. Function ϕ is the viscosity solution which satisfies the Cauchy problem (1) with $\phi_0 = \phi_0^m$ as an initial condition.

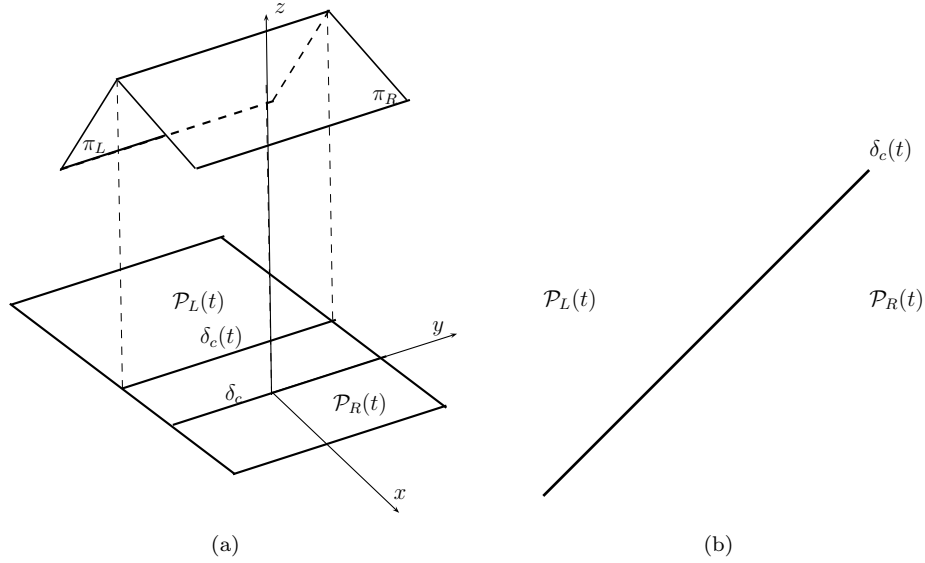(a)   (b)

Figure 7: Solution for the half-planes problem: the shock case

4.2. The rarefaction: case $F < 0$ with $\omega_0 \neq 0$. Since $\omega_0 \neq 0$, solution U of the Riemann problem (2) is a rarefaction situated in the cone $\lambda_L < \frac{\varsigma}{t} < \lambda_R$ with

$$\lambda_L = \lambda(\omega_L) = F \frac{\omega_L}{|\mathbf{U}_L|}, \qquad \lambda_R = \lambda(\omega_R) = F \frac{\omega_R}{|\mathbf{U}_R|}.$$

To describe the solution ϕ of the associated the Cauchy problem (1), we define the following lines and domains (see figure (8))

$$\delta_L(t) = \{\boldsymbol{x} \in \mathbb{R}^2; \ \boldsymbol{x}.\mathbf{W} = \lambda_L t\}, \quad \delta_R(t) = \{\boldsymbol{x} \in \mathbb{R}^2; \ \boldsymbol{x}.\mathbf{W} = \lambda_R t\},$$
$$\mathcal{P}_L(t) = \{\boldsymbol{x} \in \mathbb{R}^2; \ \boldsymbol{x}.\mathbf{W} < \lambda_L t\}, \qquad \mathcal{P}_R(t) = \{\boldsymbol{x} \in \mathbb{R}^2; \ \boldsymbol{x}.\mathbf{W} > \lambda_R t\},$$

$$\mathcal{P}_c(t) = \{\boldsymbol{x} \in \mathbb{R}^2; \ \lambda_L t < \boldsymbol{x}.\mathbf{W} < \lambda_R t\}.$$

The solution $\mathbf{U}$ for the Riemann problem is a continuous function given by

$$\mathbf{U}(\boldsymbol{x}, t) = \mathbf{U}_L = \omega_L \mathbf{W} + \omega_0 \mathbf{V}, \quad \boldsymbol{x} \in \mathcal{P}_L(t),$$
$$\mathbf{U}(\boldsymbol{x}, t) = \mathbf{U}_R = \omega_R \mathbf{W} + \omega_0 \mathbf{V}, \quad \boldsymbol{x} \in \mathcal{P}_R(t),$$
$$\mathbf{U}(\boldsymbol{x}, t) = \omega(\zeta, t)\mathbf{W} + \omega_0 \mathbf{V}, \quad \zeta = \boldsymbol{x}.\mathbf{W}, \ \boldsymbol{x} \in \mathcal{P}_c(t)$$

where function $\omega(\zeta, t)$ is given by relation (9).

On domains $\mathcal{P}_L(t)$ and $\mathcal{P}_R(t)$, function ϕ is then given by

$$\phi = \phi_L(\boldsymbol{x}, t) = \boldsymbol{x}.\mathbf{U}_L - F\,|\mathbf{U}_L|\,t, \quad \boldsymbol{x} \in \mathcal{P}_L(t),$$
$$\phi = \phi_R(\boldsymbol{x}, t) = \boldsymbol{x}.\mathbf{U}_R - F\,|\mathbf{U}_R|\,t, \quad \boldsymbol{x} \in \mathcal{P}_R(t).$$

To give the analytical expression of the solution on the band $\mathcal{P}_c(t)$, we use the change of variables ζ, η and obtain a new function $\widetilde{\phi}_c(\zeta, \eta, t) = \phi_c(\boldsymbol{x}, t)$ we have to explicit. On one hand, we have $\partial_\eta \widetilde{\phi} = \omega_0$ while on the other hand $\partial_\zeta \widetilde{\phi} = \omega(\zeta, t)$ and $\partial_t \widetilde{\phi} = -F\sqrt{\omega^2(\zeta, t) + \omega_0^2}$ with

$$\omega(\zeta, t) = -\frac{\zeta |\omega_0|}{\sqrt{t^2 F^2 - \zeta^2}}, \quad \frac{\zeta}{t} \in]\lambda_L, \lambda_R[.$$

We consider the function $\gamma(\zeta, t) = |\omega_0|\sqrt{t^2 F^2 - \zeta^2}$ and we claim that $\widetilde{\phi}_c(\zeta, \eta, t) = \gamma(\zeta, t) + \eta \omega_0$ is the solution of the problem.

We first easily check that relations $\partial_\eta \widetilde{\phi} = \omega_0$ and $\partial_\zeta \widetilde{\phi}_c = \omega(\zeta, t)$ are well-satisfied. We now check that $\widetilde{\phi}_c$ satisfies the level set equation

$$\partial_t \widetilde{\phi} = -F|\nabla_{\zeta, \eta} \widetilde{\phi}| = -F\sqrt{\omega^2(\zeta, t) + \omega_0^2}.$$

Indeed, the time derivative provides

$$\partial_t \widetilde{\phi} = \partial_t \gamma(\zeta, t) = F^2 \frac{t |\omega_0|}{\sqrt{t^2 F^2 - \zeta^2}}$$

and, in addition, one has

$$F\sqrt{\omega^2(\zeta, t) + \omega_0^2} = F\sqrt{\frac{\zeta^2 \omega_0^2}{t^2 F^2 - \zeta^2} + \omega_0^2} = -F^2 \frac{t |\omega_0|}{\sqrt{t^2 F^2 - \zeta^2}}.$$

At last, we provide the ϕ_c expression in function of the $\boldsymbol{x}$ variable:

$$\phi_c(\boldsymbol{x}, t) = |\omega_0|\sqrt{t^2 F^2 - (\boldsymbol{x} \cdot \mathbf{W})^2} + (\boldsymbol{x} \cdot \mathbf{V})\omega_0, \ \boldsymbol{x} \in \mathcal{P}_c(t).$$

To end the construction, we now prove that function ϕ is continuous on the whole domain, in particularly on line $\delta_L(t)$ and $\delta_R(t)$. Noting that line $\delta_L(t)$ is characterized in the $\mathbf{W}, \mathbf{V}$ basis by

$$\zeta = \zeta_L(t) := F\frac{\omega_L}{|\mathbf{U}_L|}t$$

and function $\widetilde{\phi}_L(\zeta, \eta, t)$ is given by

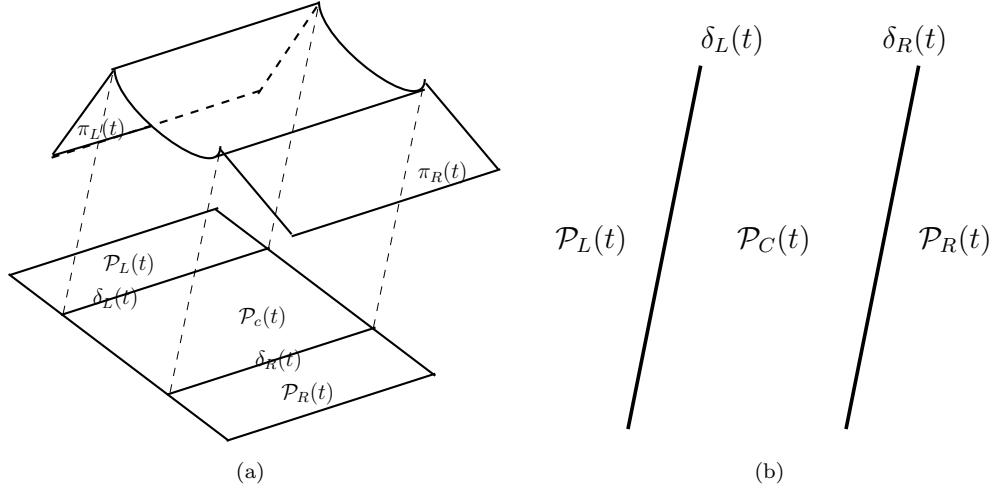$$\phi_L(\zeta, \eta, t) = \omega_L \zeta + \omega_0 \zeta - F\,|\mathbf{U}_L|\,t;$$

Figure 8: Solution for the half-planes problem: the rarefaction case with $\omega_0 \neq 0$

we then have on the line $\delta_L(t)$:

$$\widetilde{\phi}_L(\zeta_L(t), \eta, t) - \widetilde{\phi}_c(\zeta_L(t), \eta, t)$$

$$= \zeta_L(t)\omega_L + \eta\omega_0 - F\,|\mathbf{U}_L|\,t - (-|\omega_0|\sqrt{t^2F^2 - \zeta_L^2(t)} + \eta\omega_0),$$

$$= F\frac{(\omega_L)^2}{|\mathbf{U}_L|}t - F|\mathbf{U}_L|t + |\omega_0|\sqrt{t^2F^2 - \left(Ft\frac{\omega_L}{|\mathbf{U}_L|}\right)^2},$$

$$= Ft\left(\frac{\omega_L^2}{|\mathbf{U}_L|} - |\mathbf{U}_L| + \frac{|\omega_0|}{|\mathbf{U}_L|}\sqrt{|\mathbf{U}_L|^2 - \omega_L^2}\right),$$

$$= Ft\left(\frac{\omega_L^2}{|\mathbf{U}_L|} - |\mathbf{U}_L| + \frac{\omega_0^2}{|\mathbf{U}_L|}\right) = 0.$$

We deduce that function ϕ is continuous on line $\delta_L(t)$ and the result also holds on line $\delta_R(t)$

4.3. The contact discontinuity: case $F < 0$ with $\omega_0 = 0$. The rarefaction degenerates into a contact discontinuity when ω_0 tends to 0 and three situations have to be considered in functions of the ω_L and ω_R sign.

First, assume that $\omega_R < \omega_L < 0$, we denote by $\delta_c(t)$ the parallel line to δ_c given by

$$\delta_c(t) = \{\boldsymbol{x} \in \mathbb{R}^2;\ \boldsymbol{x}.\mathbf{W} = -Ft\}$$

and the two half-planes

$$\mathcal{P}_L(t) = \{\boldsymbol{x} \in \mathbb{R};\ \boldsymbol{x}.\mathbf{W} < -Ft\}, \qquad \mathcal{P}_R(t) = \{\boldsymbol{x} \in \mathbb{R};\ \boldsymbol{x}.\mathbf{W} > -Ft\}.$$

Solution $\mathbf{U}(\boldsymbol{x}, t)$ is given by

$$\mathbf{U}(\boldsymbol{x}, t) = \mathbf{U}_L, \quad \boldsymbol{x} \in \mathcal{P}_L(t),$$
$$\mathbf{U}(\boldsymbol{x}, t) = \mathbf{U}_R, \quad \boldsymbol{x} \in \mathcal{P}_R(t).$$

and the viscosity solution ϕ is the continuous Lipschitz function defined by

$$\phi(\boldsymbol{x}, t) = \boldsymbol{x}.\mathbf{U}_L - F\,|\mathbf{U}_L|\,t, \quad \boldsymbol{x} \in \mathcal{P}_L(t),$$
$$\phi(\boldsymbol{x}, t) = \boldsymbol{x}.\mathbf{U}_R - F\,|\mathbf{U}_R|\,t, \quad \boldsymbol{x} \in \mathcal{P}_R(t).$$

The case where $0 < \omega_R < \omega_L$ can be treated in the same way.

We now consider the situation where $\omega_R < 0 < \omega_L$, with $F < 0$. We define the lines

$$\delta_L(t) = \{\boldsymbol{x} \in \mathbb{R}^2;\ \boldsymbol{x}.\mathbf{W} = Ft\}, \quad \delta_R(t) = \{\boldsymbol{x} \in \mathbb{R}^2;\ \boldsymbol{x}.\mathbf{W} = -Ft\}$$

and the domain

$$\mathcal{P}_L(t) = \{\boldsymbol{x} \in \mathbb{R}^2;\ \boldsymbol{x}.\mathbf{W} < Ft\}, \qquad \mathcal{P}_R(t) = \{\boldsymbol{x} \in \mathbb{R}^2;\ \boldsymbol{x}.\mathbf{W} > -Ft\},$$

$$\mathcal{P}_c(t) = \{\boldsymbol{x} \in \mathbb{R}^2;\ Ft < \boldsymbol{x}.\mathbf{W} < -Ft\}.$$
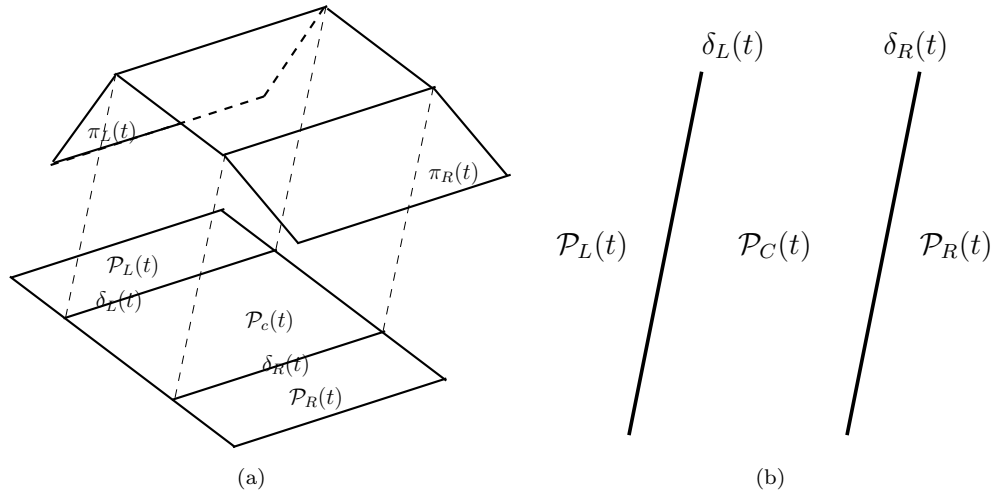

Figure 9: Solution for the half-planes problem, the rarefaction case with $\omega_0 = 0$ and $\omega_R < 0 < \omega_L$.

The solution $\mathbf{U}$ for the Riemann problem is a piecewise constant function given by

$$\begin{aligned}
\mathbf{U}(\boldsymbol{x},t) &= \mathbf{U}_L, & \boldsymbol{x} &\in \mathcal{P}_L(t), \\
\mathbf{U}(\boldsymbol{x},t) &= \mathbf{U}_R, & \boldsymbol{x} &\in \mathcal{P}_R(t), \\
\mathbf{U}(\boldsymbol{x},t) &= 0, & \boldsymbol{x} &\in \mathcal{P}_c(t)
\end{aligned}$$

and the viscosity solution ϕ is the continuous Lipschitz function defined by

$$\begin{aligned}
\phi &= \phi_L(\boldsymbol{x},t) = \boldsymbol{x}.\mathbf{U}_L - F\,|\mathbf{U}_L|\,t, & \boldsymbol{x} &\in \mathcal{P}_L(t), \\
\phi &= \phi_R(\boldsymbol{x},t) = \boldsymbol{x}.\mathbf{U}_R - F\,|\mathbf{U}_R|\,t, & \boldsymbol{x} &\in \mathcal{P}_R(t), \\
\phi &= 0, & \boldsymbol{x} &\in \mathcal{P}_c(t).
\end{aligned}$$

The function is clearly continuous on the whole domain $\mathbb{R}^2$ by definition of the lines $\delta_L(t)$ and $\delta_R(t)$.

Remark 4.1. *The contact discontinuity solution comes from the monotony principle of the viscosity solution for the Hamilton-Jacobi problem in one-space dimension, equivalent to the entropy condition applied to the one-dimensional problem* (6). *The solution for $\omega_0 = 0$ is obtained as the uniform limit on $\mathbb{R}^2 \times [0,T]$ of a Lipschitz function sequence (ϕ_{ω_0}) where ϕ_{ω_0} are the viscosity solutions of the level set equation with $\omega_0 > 0$.*

5. Numerical tests

The goal of this section is to compare the analytical solution proposed in section 4 with numerical approximations using the classical schemes on structured grids (see [8] for a survey). We focus our study on the simple level set equation

(10)
$$\begin{cases} \partial_t \phi(\boldsymbol{x}, t) + F\,|\nabla\phi(\boldsymbol{x}, t)| = 0 & \text{in } \Omega \times [0, T], \\ \phi(\boldsymbol{x}, t = 0) = \phi_0(\boldsymbol{x}) & \text{in } \Omega, \\ \dfrac{\partial\phi}{\partial\boldsymbol{n}} = 0 & \text{on } \partial\Omega \times [0, T]. \end{cases}$$

where $\Omega = [a, b] \times [a, b]$ with $a < b$, $T > 0$, $F \in \mathbb{R}$ and

$$\phi_0(\boldsymbol{x}) = \phi_0^m(\boldsymbol{x}) = \min(\mathbf{U}_1.\boldsymbol{x}, \mathbf{U}_2.\boldsymbol{x})$$

such that $\mathbf{U}_1, \mathbf{U}_2$ are two prescribed vectors of $\mathbb{R}^2$.

5.1. Discretization on a Cartesian grid. Let $I \in \mathbb{N}^*$, we define a uniform mesh of Ω with space step $\Delta\boldsymbol{x} = \dfrac{b-a}{I}$ and nodes

$$\boldsymbol{x}_{i,j} = (a + i\Delta x, b + j\Delta x), \quad 0 \le i, j \le I.$$

Let $N \in \mathbb{N}^*$, we denote by $(t^n)_{n=0,\ldots,L}$ a subdivision of the time interval $[0, T]$, with $\Delta t^n = t^{n+1} - t^n$ the time step (the subdivision is not uniform) and the maximum time step by

$$\Delta t = \max_{n=1,\ldots,N} \Delta t^n.$$

Let $\phi_{i,j}^n$ be an approximation of $\phi(\boldsymbol{x}_{i,j}, t^n)$ for all $i, j = 0, \ldots, L$ at time t^n, then we compute an approximation at time t^{n+1} using the scheme (see [8]):

(11)
$$\phi_{i,j}^{n+1} = \phi_{i,j}^n - F\frac{\Delta t^n}{\Delta\boldsymbol{x}}(\max(F, 0)\nabla^+ + \min(F, 0)\nabla^-), \ i, j = 0, \ldots, I$$

where we define

$$\nabla^+ = \left(\max(\phi_{i,j}^n - \phi_{i-1,j}^n, 0)^2 + \min(\phi_{i+1,j}^n - \phi_{i,j}^n, 0)^2 + \right.$$
$$\left. \max(\phi_{i,j}^n - \phi_{i,j-1}^n, 0)^2 + \min(\phi_{i,j+1}^n - \phi_{i,j}^n, 0)^2\right)^{\frac{1}{2}},$$
$$\nabla^- = \left(\min(\phi_{i,j}^n - \phi_{i-1,j}^n, 0)^2 + \max(\phi_{i+1,j}^n - \phi_{i,j}^n, 0)^2 + \right.$$
$$\left. \min(\phi_{i,j}^n - \phi_{i,j-1}^n, 0)^2 + \max(\phi_{i,j+1}^n - \phi_{i,j}^n, 0)^2\right)^{\frac{1}{2}}.$$

The maximum time step length is controlled by the Courant-Lax-Friedrisch condition (CFL) $\Delta t \le \dfrac{\Delta\boldsymbol{x}}{|F|} \times \mathbf{cfl}$ where $\mathbf{cfl} \in [0, 1]$ is a parameter we use to reduce the time step. The discrete L^1-norm and L^∞-norm at time t^n are given by

$$\varepsilon^1(t^n) = \sum_{i,j} |\phi_{ij}^n - \phi^e(\boldsymbol{x}_{ij}, t^n)|\Delta x, \quad \varepsilon^\infty(t^n) = \max_{i,j} |\phi_{ij}^n - \phi^e(\boldsymbol{x}_{ij}, t^n)|.$$

where ϕ_{ij}^e is the analytical solution.

All the numerical experiments have been carried out with $\Omega = [-1, 1]^2$ and five grids $\mathcal{T}_k$ of space step $\Delta_k x = \dfrac{2^{1-k}}{10}$, $k = 1, \ldots, 5$ have been employed to measure the convergence rate.

Let $\mathbf{U}_L$ and $\mathbf{U}_R$ be two prescribed vectors of $\mathbb{R}^2$, we then evaluate vector $\mathbf{W}$ with (3) and the half-planes $\mathcal{P}_L, \mathcal{P}_R$. We define the initial condition for the Cauchy problem

$$\phi_0(\boldsymbol{x}) = \min(\mathbf{U}_L.\boldsymbol{x}, \mathbf{U}_R.\boldsymbol{x}).$$

Note that by construction we have $\nabla\phi_0 = \mathbf{U}_L$ on $\mathcal{P}_L$ and $\nabla\phi_0 = \mathbf{U}_R$ on $\mathcal{P}_R$.

5.2. The shock case: $F > 0$. We set $F = 1$ and consider two situations whether ω_0 is null or not. We first choose $\mathbf{U}_L = \begin{pmatrix} -2 \\ 1 \end{pmatrix}$, $\mathbf{U}_R = \begin{pmatrix} 1 \\ 1 \end{pmatrix}$ then we have $\mathbf{W} = \begin{pmatrix} -1 \\ 0 \end{pmatrix}$ and $\omega_0 = 1$. The analytical solution of the problem (10) is given by

$$\phi(x, y, t) = \begin{cases} -2x + y + \sqrt{5}t, & -x < \frac{\sqrt{5} - \sqrt{2}}{3}t, \\ x + y + \sqrt{2}t, & -x > \frac{\sqrt{5} - \sqrt{2}}{3}t. \end{cases}$$

For the second case, we choose $\mathbf{U}_L = \begin{pmatrix} -1 \\ 0 \end{pmatrix}$, $\mathbf{U}_R = \begin{pmatrix} 2 \\ 0 \end{pmatrix}$ then we have $\mathbf{W} = \begin{pmatrix} -1 \\ 0 \end{pmatrix}$ and $\omega_0 = 0$. The analytical solution of the problem (10) is given by

$$\phi(x, y, t) = \begin{cases} -x + t, & -x < \frac{1 - \sqrt{2}}{3}t, \\ 2x + \sqrt{2}t, & -x > \frac{1 - \sqrt{2}}{3}t. \end{cases}$$

We display in figure (10) a comparison between the analytical solution and the numerical solution at time $t = 0.5$ computing with mesh $\mathcal{T}_3$ both for the case $\omega_0 \neq 0$ and the case $\omega_0 = 0$. The curves correspond to the planar cut of ϕ in the $\mathbf{W}$ direction. Convergence rates in L^1-norm and L^∞-norm are given in table (1). We observe that the numerical approximation suit well with the analytical solution and we obtain an effective second-order convergence between the approximation and the exact solution.

(a) $\omega_0 \neq 0$

(b) $\omega_0 = 0$
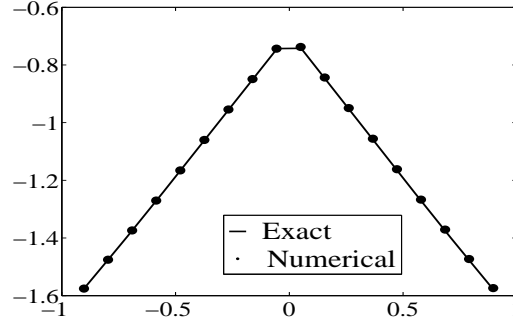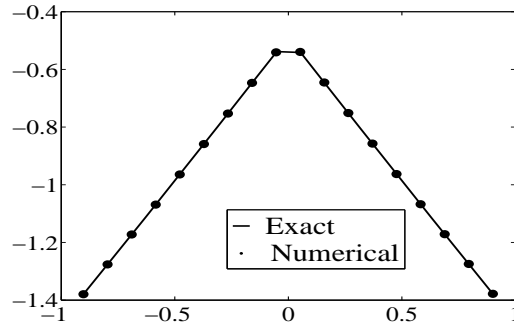
Figure 10: ϕ curve in the $\mathbf{W}$ direction at time $t = 0.5$: the shock case with $\omega_0 \neq 0$ (left) and $\omega_0 = 0$ (right).

(a) $\omega_0 \neq 0$

Δx	L^1 error	order	L^∞ error	order
0.2	4.40 $\times 10^{-2}$	-	7.66 $\times 10^{-2}$	-
0.1	2.45 $\times 10^{-2}$	1.79	3.71 $\times 10^{-2}$	2.06
0.05	1.28 $\times 10^{-2}$	1.91	1.81 $\times 10^{-2}$	2.04
0.025	6.55 $\times 10^{-3}$	1.95	8.95 $\times 10^{-3}$	2.02
0.0125	3.30 $\times 10^{-3}$	1.98	4.44 $\times 10^{-3}$	2.01

(b) $\omega_0 = 0$

Δx	L^1 error	order	L^∞ error	order
0.2	3.06 $\times 10^{-2}$	-	5.18 $\times 10^{-2}$	-
0.1	1.70 $\times 10^{-2}$	1.80	2.60 $\times 10^{-2}$	1.99
0.05	8.97 $\times 10^{-3}$	1.89	1.28 $\times 10^{-2}$	2.03
0.025	4.58 $\times 10^{-3}$	1.95	6.32 $\times 10^{-3}$	2.02
0.0125	2.31 $\times 10^{-3}$	1.98	3.14 $\times 10^{-3}$	2.01

Table 1: *Convergence rate for the shock cases: $\omega_0 \neq 0$ (top) and $\omega_0 = 0$ (bottom).*

5.3. The rarefaction case: $F < 0$ and $\omega_0 \neq 0$. We set $F = -1$ and we choose $\mathbf{U}_L = \begin{pmatrix} 1 \\ 0 \end{pmatrix}$, $\mathbf{U}_R = \begin{pmatrix} 1 \\ 1 \end{pmatrix}$ then we have $\mathbf{W} = \begin{pmatrix} 0 \\ -1 \end{pmatrix}$ and $\omega_0 = -1$. The analytical solution of problem (10) is given by

$$\phi(x, y, t) = \begin{cases} x + t, & -x < t, \\ x + y + \sqrt{2}t, & -x > \frac{t}{\sqrt{2}}, \\ \sqrt{t^2 - x^2} + y, & t < -x < \frac{t}{\sqrt{2}}. \end{cases}$$

We show in figure (11) a comparison between the analytical solution and the numerical solution at time $t = 0.5$ computing with mesh $\mathcal{T}_3$ where the curves correspond to the planar cut of ϕ in the $\mathbf{W}$ direction. Convergence rates in L^1-norm and L^∞-norm are given in table (2). Again, we observe a nice correspondence between the numerical approximation and the analytical solution confirmed by the effective second-order convergence between the approximation and the exact solution.

(a) $\omega_0 \neq 0$
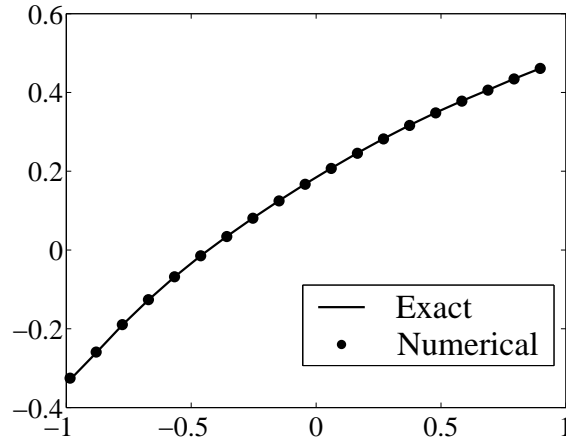
Figure 11: *ϕ curve in the $\mathbf{W}$ direction at time $t = 0.5$: the rarefaction case with $\omega_0 \neq 0$.*

(a) $\omega_0 \neq 0$

Δx	L^1 error	order	L^∞ error	order
0.2	4.18×10^{-2}	-	9.68×10^{-2}	-
0.1	2.36×10^{-2}	1.77	5.63×10^{-2}	1.71
0.05	1.25×10^{-2}	1.88	3.29×10^{-2}	1.71
0.025	6.66×10^{-3}	1.87	1.93×10^{-2}	1.70
0.0125	3.86×10^{-3}	1.72	1.13×10^{-2}	1.70

Table 2: *Convergence rate for the rarefaction ($\omega_0 \neq 0$ case).*

5.4. The contact discontinuity case: $F < 0$ and $\omega_0 = 0$. We set $F = -1$ and choose $\mathbf{U}_L$ and $\mathbf{U}_R$ such as $\omega_0 = 0$. Two cases arise whether $\omega_L \omega_R > 0$ or $\omega_L \omega_R < 0$.
We first choose $\mathbf{U}_L = \begin{pmatrix} 1 \\ 0 \end{pmatrix}$, $\mathbf{U}_R = \begin{pmatrix} 2 \\ 0 \end{pmatrix}$ then we have $\mathbf{W} = \begin{pmatrix} -1 \\ 0 \end{pmatrix}$ and $\omega_L = -1$, $\omega_R = -2$, $\omega_0 = 0$. The analytical solution of problem (10) is given by

$$\phi(x, y, t) = \begin{cases} x + t, & -x < t, \\ 2x + 2t, & -x > t. \end{cases}$$

for the second case, we choose $\mathbf{U}_L = \begin{pmatrix} 1 \\ 0 \end{pmatrix}$, $\mathbf{U}_R = \begin{pmatrix} -1 \\ 0 \end{pmatrix}$ then we have $\mathbf{W} = \begin{pmatrix} 1 \\ 0 \end{pmatrix}$ and $\omega_L = 2$, $\omega_R = 1$, $\omega_0 = 0$. The analytical solution of problem (10) is given by

$$\phi(x, y, t) = \begin{cases} x + t, & \frac{2}{\sqrt{2}}x < -t, \\ -x + t, & \frac{2}{\sqrt{2}}x > t, \\ 0, & -t < \frac{2}{\sqrt{2}}x < t. \end{cases}$$

We show in figure (12) a comparison between the analytical solution and the numerical solution at time $t = 0.5$ computing with mesh $\mathcal{T}_3$ both for the case $\omega_L \omega_R > 0$ and the case $\omega_L \omega_R < 0$. The curves correspond to the planar cut of ϕ in the $\mathbf{W}$ direction. Convergence rates in L^1-norm and L^∞-norm are given in table (3). We obtain a very good approximation of the analytical solution confirmed by the effective second-order convergences between the approximation and the exact solution.
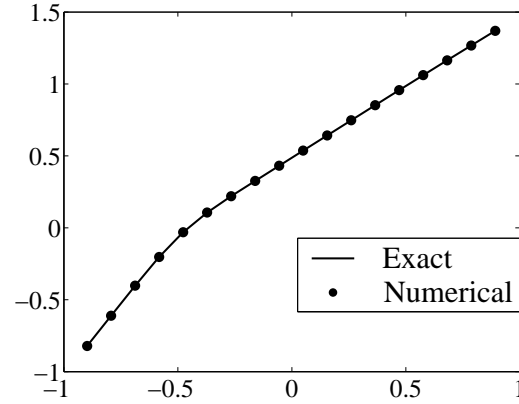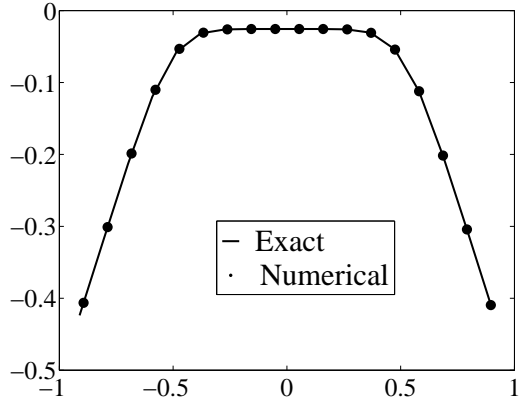
(a) $\omega_L\omega_R > 0$

(b) $\omega_L\omega_R < 0$

Figure 12: ϕ curve in the **W** direction at time $t = 0.5$: the contact discontinuity case with $\omega_L\omega_R > 0$ (left) and $\omega_L\omega_R < 0$ (right).

(a) $\omega_L\omega_R > 0$

Δx	L^1 error	order	L^∞ error	order
0.2	2.80×10^{-2}	-	5.18×10^{-2}	-
0.1	1.95×10^{-2}	1.43	4.39×10^{-2}	1.17
0.05	1.18×10^{-2}	1.62	2.56×10^{-2}	1.25
0.025	6.54×10^{-3}	1.74	1.26×10^{-2}	1.17
0.0125	3.39×10^{-3}	1.92	6.29×10^{-3}	2.00

(b) $\omega_L\omega_R < 0$

Δx	L^1 error	order	L^∞ error	order
0.2	4.23×10^{-2}	-	1.11×10^{-1}	-
0.1	2.67×10^{-2}	1.68	5.50×10^{-2}	2.01
0.05	1.45×10^{-2}	1.71	3.26×10^{-2}	1.68
0.025	7.63×10^{-3}	1.82	2.30×10^{-2}	1.41
0.0125	3.95×10^{-3}	1.93	1.61×10^{-2}	1.42

Table 3: Convergence rate for the contact discontinuity: case $\omega_L\omega_R > 0$ (top) and case $\omega_L\omega_R < 0$ (bottom).

6. Conclusion

We have determined the analytical solution of Cauchy problem for the level set equation when the initial data is composed of two half-planes. Such a problem corresponds to the Riemann problem in the hyperbolic system context and may be helpful to test numerical schemes for level set equation. We show that we have three configurations corresponding to the entropic shock, the rarefaction and the contact discontinuity which is the limit case of the rarefaction with $\omega_0 = 0$. Numerical simulations have been performed using a classical method on structured grids to compare with the analytical solution in the three cases and we obtain an effective second-order convergence. Extension for the general Hamilton-Jacobi problem can be considered and a "Riemann solver" for level set equation based on the two half-planes problem may also be investigated.

References

[1] Guy Barles. *Solutions de viscosité des équations de Hamilton-Jacobi*, volume 17 of *Mathématiques & Applications (Berlin) [Mathematics & Applications]*. Springer-Verlag, Paris, 1994.

[2] L. Corrias, M. Falcone, and R. Natalini. Numerical schemes for conservation laws via Hamilton-Jacobi equations. *Math. Comp.*, 64(210):555–580, S13–S18, 1995.

[3] Michael G. Crandall and Pierre-Louis Lions. Viscosity solutions of Hamilton-Jacobi equations. *Trans. Amer. Math. Soc.*, 277(1):1–42, 1983.

[4] Stéphane Clain. A simple level set numerical scheme for unstructured meshes. In *Finite volumes for complex applications, III (Porquerolles, 2002)*, pages 295–302. Hermes Sci. Publ., Paris, 2002.

[5] Malcom Djenno. *Nouvelles approximations numériques pour les équations de Stokes et l'équation Level Set*. Thèse de doctorat, université Blaise-Pascal, 2007.

[6] Randall J. LeVeque. *Numerical methods for conservation laws*. Lectures in Mathematics ETH Zürich. Birkhäuser Verlag, Basel, second edition, 1992.

[7] Pierre-Louis Lions. *Generalized solutions of Hamilton-Jacobi equations*, volume 69 of *Research Notes in Mathematics*. Pitman (Advanced Publishing Program), Boston, Mass., 1982.

[8] J. A. Sethian. *Level set methods*, volume 3 of *Cambridge Monographs on Applied and Computational Mathematics*. Cambridge University Press, Cambridge, 1996. Evolving interfaces in geometry, fluid mechanics, computer vision, and materials science.

Departamento de Matemática e Aplicações, Centro de Matemática, Campus de Gualtar - 4710-057 Braga Campus de Azurém- 4800-058 Guimaraẽs, Portugal

E-mail: `clain@math.uminho.pt`

Laboratoire de mathématiques, CNRS UMR 6620, Université Blaise Pascal,, BP 10448, F-63000 Clermont-Ferrand, France, and Université des Sciences et Techniques de Masuku (USTM),, B.P 941 Franceville, Gabon.

E-mail: `djenno@math.univ-bpclermont.fr`